Am J Physiol Regul Integr Comp Physiol 290: R1460–R1467, 2006.
First published January 5, 2006; doi:10.1152/ajpregu.00806.2005.

Alteration of copper physiology in mice overexpressing the human Menkes protein ATP7A

Bi-Xia Ke,* Roxana M. Llanos,* Magali Wright, Yolanda Deal, and Julian F. B. Mercer

Centre for Cellular and Molecular Biology, School of Life and Environmental Sciences, Deakin University, Burwood, Victoria, Australia

Submitted 15 November 2005; accepted in final form 24 December 2005

Ke, Bi-Xia, Roxana M. Llanos, Magali Wright, Yolanda Deal, and Julian F. B. Mercer. Alteration of copper physiology in mice overexpressing the human Menkes protein ATP7A. *Am J Physiol Regul Integr Comp Physiol* 290: R1460–R1467, 2006. First published January 5, 2006; doi:10.1152/ajpregu.00806.2005.—The Menkes protein (ATP7A) is defective in the Cu deficiency disorder Menkes disease and is an important contributor to the maintenance of physiological Cu homeostasis. To investigate more fully the role of ATP7A, transgenic mice expressing the human Menkes gene *ATP7A* from chicken β-actin composite promoter (CAG) were produced. The transgenic mice expressed ATP7A in lung, heart, liver, kidney, small intestine, and brain but displayed no overt phenotype resulting from expression of the human protein. Immunohistochemical analysis revealed that ATP7A was found primarily in the cardiac muscle, smooth muscle of the lung, distal tubules of the kidney, intestinal enterocytes, and patches of hepatocytes, as well as in the hippocampus, cerebellum, and choroid plexus of the brain. In 60-day- and 300-day-old mice, Cu concentrations were reduced in most tissues, consistent with ATP7A playing a role in Cu efflux. The reduction in Cu was most pronounced in the hearts of older T22#2 females (24%), T22#2 males (18%), and T25#5 females (23%), as well as in the brains of 60-day-old T22#2 females and males (23% and 30%, respectively).

copper homeostasis; transgenic mice

TISSUE COPPER CONCENTRATIONS and distribution in the body must be tightly controlled to ensure delivery of Cu to essential cuproenzymes such as cytochrome *c* oxidase and lysyl oxidase without causing toxicity as a result of the formation of free radicals promoted by free Cu ions. Background literature concerning Cu homeostasis is discussed in detail by Linder (17). The importance of Cu homeostatic mechanisms is graphically demonstrated by the severity of the genetic disorders of Cu homeostasis: Menkes and Wilson diseases. Menkes disease is a fatal X-linked Cu-deficiency disorder that presents with a wide range of symptoms, including neurodegeneration, connective tissue defects, and abnormal hair. Most patients with Menkes disease die in early childhood and have abnormally low Cu concentrations in many tissues, such as brain, liver, and heart, but paradoxically some tissues accumulate Cu (e.g., kidney, small intestine) (8). Wilson disease is an autosomal recessive Cu toxicity disorder in which Cu accumulates to extremely high concentrations in the liver and can result in liver failure or neurological defects caused by Cu deposits in the central nervous system. Wilson disease is potentially fatal but can be treated with Cu chelators (8, 17).

The identification of the genes affected in Menkes disease (5, 21, 37) and Wilson disease (3, 33, 39) provided the first important insights into the molecular basis of Cu homeostasis. These genes encode closely related Cu-transporting P-type ATPases with 67% amino acid identity (2). The Menkes gene, *ATP7A*, encodes the Menkes protein ATP7A, and the Wilson gene, *ATP7B*, encodes the Wilson protein ATP7B. Many disease-causing mutations have been found in both genes and in most cases are predicted to abolish almost completely the Cu-transporting activity of the proteins (35, 36). The distinct clinical presentation of the two diseases suggests that ATP7A and ATP7B have different physiological roles in Cu homeostasis. The pattern of expression of the two genes provides some indication of their physiological roles and the clinical effects of the mutations. ATP7A is expressed in many tissues, with the notable exception of the hepatocytes (26, 37), whereas ATP7B is expressed predominantly in the liver and to a more limited extent in brain, placenta, and kidney (3, 33). Overall, it appears that the two ATPases have evolved to possess distinct physiological roles in Cu homeostasis. The Menkes protein is essential not only for efficient dietary Cu uptake in the small intestine but also in the delivery of Cu to the brain across the blood-brain barrier and recovery of Cu from the proximal tubules of the kidney. The fact that cells from patients with Menkes disease have defective Cu efflux suggests that ATP7A is necessary for Cu export from cells (13). The expression of ATP7B in the liver and the massive accumulation of Cu in this organ in Wilson disease suggests that ATP7B is essential for the excretion of Cu from the liver. In mammals, overall physiological Cu balance is maintained largely by excretion of excess Cu in the bile (18). Most cell types express only ATP7A or ATP7B but not both; however, placental trophoblasts and mammary epithelial cells express both, which may reflect the importance of correct Cu delivery to the fetus and growing neonate (1, 12). Both ATPases also have a role in the delivery of Cu to secreted cuproenzymes; ATP7A delivers Cu to lysyl oxidase (15), and ATP7B supplies Cu to ceruloplasmin (34).

Both ATP7A and ATP7B undergo Cu-induced trafficking when cells in culture are exposed to excess Cu. In normal Cu conditions, both ATPases are located in the *trans*-Golgi network, where they supply Cu to secreted cuproenzymes (29, 34). When intracellular Cu concentrations rise, ATP7A traffics to the plasma membrane (28), thus facilitating the export of excess Cu. Similarly, ATP7B in hepatocytes traffics to endosome-like vesicles and may also reach the apical surface of the hepatocytes (30, 31). The Cu-induced trafficking of these

* B.-X. Ke and R. M. Llanos contributed equally to this work.

Address for reprint requests and other correspondence: J. F. B. Mercer, Centre for Cellular and Molecular Biology, School of Life and Environmental Sciences, Deakin University, Bldg. L, 221 Burwood Highway, Burwood, Victoria 3052, Australia (e-mail: jmercer@deakin.edu.au).

The costs of publication of this article were defrayed in part by the payment of page charges. The article must therefore be hereby marked "*advertisement*" in accordance with 18 U.S.C. Section 1734 solely to indicate this fact.

ATPases has been proposed to be fundamental to cellular Cu homeostasis and to be largely responsible for the maintenance of systemic Cu levels within safe limits (20). Although many studies have investigated the trafficking of these proteins in cultured cells, less is known about the role of trafficking of the ATPases in the whole animal. The location of ATP7A has been shown to be altered during lactation (1), and Cu exposure of mice has been demonstrated to induce relocation of ATP7B from the *trans*-Golgi to large vesicles in hepatocytes (31). However, studies have been limited by the difficulty in detecting the protein in many cell types because of its low expression levels.

To further extend knowledge of the role of ATP7A in mammalian Cu homeostasis, we generated transgenic mice in which ATP7A was overexpressed. The transgene is controlled by a constitutive, ubiquitously expressed promoter derived from a modified chicken β-actin composite promoter (CAG) (25). The overall phenotype of transgenic mice was normal, and the transgene was transmissible to progeny, but the transgenic mice showed interesting changes in Cu concentration in various organs that were generally consistent with a role for ATP7A in efflux.

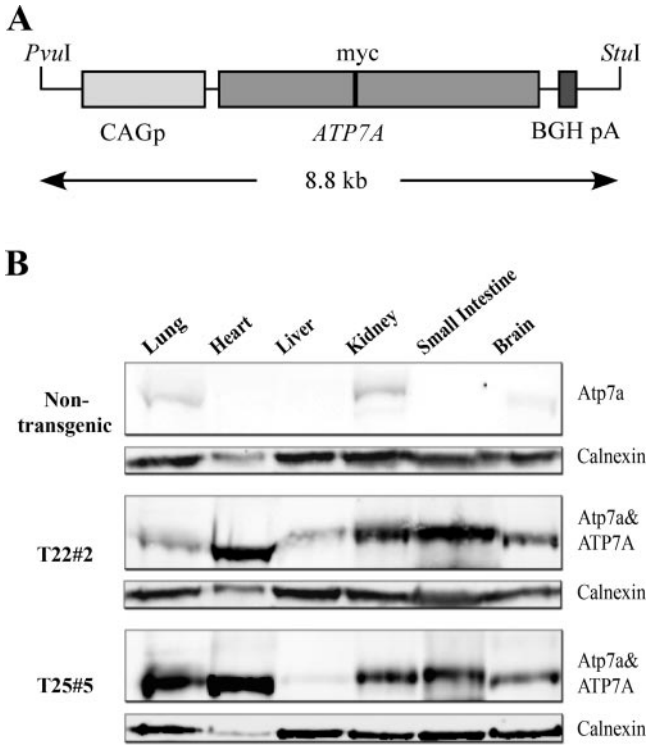

Fig. 1. Generation of chicken β-actin composite promoter (CAG)-*ATP7A* (Menkes protein) transgenic mice. *A*: schematic of the CAG-*ATP7A* construct. *ATP7A* represents the *ATP7A* coding region with a myc epitope (27), and BGH pA represents the bovine growth hormone polyadenylation signal. *B*: representative Western blot analysis of nontransgenic mice (*top*). R17-BX antibody detected ATP7A (178 kDa) in lysates from lung, heart, spleen, kidney, small intestine, and brain in the T22#2 line (*middle*) and the T25#5 line (*bottom*). Calnexin antibody was used as an indication of protein loading.

MATERIALS AND METHODS

Animals. All animal protocols were performed in accordance with the Deakin University Animal Welfare Committee regulations, approval numbers A1/1999 and A20/2001. All mice used in this study were maintained on a 12-h light/12-h dark cycle. The transgenic mice were produced in the C57BL/6 background.

Generation of the transgenic mice. The mammalian expression vector pcDNA3 (Invitrogen, Carlsbad, CA) was modified by replacing its origin of replication with that from pWSK29 (38). Furthermore, the cytomegalovirus (CMV) promoter was replaced with the CAG promoter (25) to generate the plasmid pCMB336. The myc-tagged *ATP7A* cDNA (27) was inserted into the *Eco*RV/*Xho*I restriction enzyme sites of pCMB336 generating plasmid pCMB344. An 8.8-kb *Pvu*I/*Stu*I fragment containing CAG-*ATP7A*-bovine growth hormone poly(A) signal (Fig. 1*A*) was used at 2 ng/ml for pronuclear microinjection (Mouseworks, Monash University, Melbourne, Victoria, Australia).

Screening of transgenic lines. Mice were genotyped by PCR of tail DNA using two primer sets: *1*) sense oligonucleotide Y2H7 (5′-TCTCTCTTCCTTAAACTTTAC-3′) corresponding to the 3′-end sequence of *ATP7A*, and the antisense oligonucleotide SP6 (5′-ATTTAGGTGACACTATAG-3′) from the vector; and *2*) *ATP7A* 9A (5′-ATTCTGTTACCATTTCTGTTGAG-3′) and 63C (5′-CATCTTCAGCACGACTTCACC-3′) from the human *ATP7A* sequence. PCR conditions were 95°C for 3 min for one cycle, followed by 30 cycles of 94°C for 30 s, 56°C for 1 min, and 72°C for 1 min. Animals shown to be transgenic were subsequently mated with wild-type C57BL/6 mice. Transgenic lines were maintained as heterozygotes.

Antibodies. Despite the inclusion of the myc epitope in the ATP7A construct, the myc antibody did not prove reliable for detecting ATP7A in the transgenic mice. Therefore, we used antibodies raised to ATP7A that detected both endogenous and transgenic proteins. The ATP7A antibodies were raised in sheep against the first 590 NH_2-terminal amino acids consisting of the six Cu-binding domains fused to a $(His)_6$ tag at the NH_2 terminus. Affinity-purified antibody (R17-BX) was isolated from the sodium sulfate IgG-precipitated fraction by performing immunoaffinity chromatography using the 590 NH_2-terminal amino acids of ATP7A coupled to cyanogen bromide-activated beads (Sigma-Aldrich, Castle Hill, NSW, Australia).

Western blot analysis. Mice (60 days old) were killed by CO_2 asphyxiation, and various tissues (lung, heart, liver, kidney, small intestine, and brain) were collected and frozen immediately on dry ice. Tissues were ground in liquid nitrogen with mortar and pestle and homogenized in extraction buffer containing 6% SDS, 0.14 M Tris·HCl, pH 6.8, and 22.4% glycerol with protease inhibitors (Complete Mini EDTA-free protease inhibitor cocktail tablets; Roche Diagnostics, Castle Hill, Australia). DNA in the tissues was sheared by passing through 18-, 21-, and 25-gauge needles. The total protein content was determined using the bicinchoninic acid method (Pierce, Rockford, IL) according to the manufacturer's instructions. Proteins (80 μg) were electrophoresed on a 7.5% SDS-PAGE gel and transferred onto HyBond C nitrocellulose membranes (Amersham Biosciences, Little Chalfont, UK). Membranes were incubated with the R17-BX antibody (1:2,000 dilution) or anti-calnexin polyclonal Ab (1:500 dilution; Santa Cruz Biotechnology, Santa Cruz, CA) in Tris-buffered saline (TBS) containing 1% skim milk (instant skim milk powder; Diploma, Melbourne, Australia) for 1 h at room temperature. Membranes were then washed with TBS containing 1% skim milk and incubated for 1 h at room temperature with peroxidase-conjugated anti-goat IgG (1:4,000 dilution; Sigma, St. Louis, MO) or with anti-rabbit IgG (1:4,000 dilution; Chemicon International, Melbourne, Australia) in TBS containing 1% skim milk proteins and were detected using chemiluminescence (Lumi-Light Western blotting substrate; Roche Diagnostics). Densitometry to quantify results was performed using MultiGauge version 2.2 software (Fujifilm, Tokyo, Japan).

Real-time quantitative PCR. Total RNA was isolated from 60-day-old T22#2 and T25#5 mouse tissues using the RNeasy Mini Kit (Qiagen, Melbourne, Victoria, Australia). cDNA was generated from 5 μg of RNA using StrataScript RT (Stratagene, East Kew, Australia) and random primers (Roche Diagnostics). Real-time PCR was per-

formed with 1× SYBR Green PCR Master Mix (Applied Biosystems, Warrington, UK), 3 μM concentrations of forward and reverse primers for *Atp7a* (5′-AAACCTTGCGAGAAGCAATTG-3′ and 5′-GGGCAAAAGAGGTGTTTCCA-3′) and *ATP7A* (5′-GCTACCTTGTCAGACACGAATGAG-3′ and 5′-TCTTGAACTGGTGTCATCCCTTT-3′) and 20 ng of cDNA. Samples were analyzed in triplicate in 20-μl total volume using 7500 System software (Applied Biosystems). Both *Atp7a* and *ATP7A* were detected in the same transgenic tissues. The abundance of each mRNA, measured as the threshold cycle value (C_t), was calculated after each reaction. The relative RNA expression level of each sample was calculated using the equation $2^{-\Delta Ct}$, where ΔC_t is the difference between *Atp7a* and *ATP7A*.

Preparation of tissue for immunohistochemistry. Sixty-day-old animals were killed by CO_2 asphyxiation, and their organs were collected immediately. Kidney, heart, and lung were immersion fixed for 5 h, and brain was fixed for 24 h in 4% paraformaldehyde-PBS. Tissues were embedded in paraffin, sectioned at 4 μm (brain 7 μm) on a microtome HM330 (Microm, Heidelberg, Germany), and mounted onto SuperFrost slides (Menzel Glaser, Braunschweig, Germany). The paraffin-embedded sections were dewaxed, rehydrated, and microwaved to expose the epitope (7). The small intestine and liver were embedded in Tissue-Tek optimal cutting temperature compound (Sakura Finetechnical, Tokyo, Japan) and sectioned at 4 μm on a Leica CM 1850 cryostat (Leica Microsystems, Nussloch, Germany). Frozen sections were fixed in 4% paraformaldehyde-PBS and then washed with PBS.

Immunohistochemical analysis. All tissue sections were treated with 3% H_2O_2 in H_2O for 10 min to inactivate endogenous peroxidase. After being washed, sections were blocked in 1% normal rabbit serum at room temperature for 1 h. An avidin-biotin blocking kit (Vector Laboratories, Burlingame, CA) was applied to the liver sections to block the endogenous biotin and actin before serum blocking. Sections were then incubated for 1 h at room temperature with R17-BX (1:2,000 and 1:1,000 dilutions for liver sections). The signal was amplified according to the protocol provided with the Vector ABC kit (Vector Laboratories, Burlingame, CA). Color was developed using the Nova Red substrate (Vector Laboratories). Sections were counterstained with Harris's hematoxylin and mounted with DPX neutral mounting medium (Chem-Supply, Gillman, SA, Australia).

Atomic absorption spectrophotometry. Tissues were analyzed for Cu using atomic absorption spectrophotometry. Tissues were dried at 85°C for 1 wk, weighed, transferred into acid-washed tubes, and digested with 0.5 ml of nitric acid at room temperature for 1 h and then at 65°C for 3 h. After this step, 2.5 ml of double-distilled water was added. Undigested tissues were sedimented at 1,500 rpm for 5 min, and the supernatant was analyzed using a Varian GTA 100 atomic absorption spectrophotometer (Mulgrave, Australia) by direct aspiration with an air-acetylene flame. Results were expressed as micrograms per gram of dry weight.

Statistical analysis. Data are presented as means with SDs. Statistical analyses were performed using Student's two tailed *t*-test. Where the distribution of data was nonparametric, the Mann-Whitney *U*-test was used to analyze the data.

RESULTS

CAG-ATP7A construct. Our previous studies of the expression of ATP7A from a cDNA construct in cultured mammalian cell had shown a low expression frequency (16), so we were concerned that expression of the transgene from the original construct in mice would be low and variable. Modified expression constructs were prepared using pcDNA3 (Invitrogen), and the frequency of expression after transient transfection into cultured cells was assessed using indirect immunofluorescence with the R17-BX antibody. The best results were obtained with a construct (CAG-*ATP7A*, pCMB344) in which the *ATP7A* cDNA was regulated by the CAG promoter (25) prepared as described in MATERIALS AND METHODS. Using pCMB344, ~20% of cells were found to express ATP7A (data not shown). Because this frequency was a 20-fold improvement over our initial constructs, we considered this construct to be suitable for the production of transgenic mice.

Generation of ATP7A transgenic mouse lines. An 8.8-kb *Pvu*I/*Stu*I fragment containing the expression cassette (Fig. 1*A*) was introduced into one cell stage embryos by pronuclear injection, and the two cell stage embryos were transferred to recipient females using standard procedures. Potential *ATP7A* transgenic (CAG-*ATP7A*) founder mice were screened by performing PCR of genomic DNA from tail biopsies as described in MATERIALS AND METHODS. Ten independent CAG-*ATP7A* founders were identified from 22 pups born. Breeding colonies were established from a number of these founders by mating them with C57BL/6 mice. Two lines, T22#2 and T25#5, were selected for detailed analysis. Homozygote T25#5 females could not be generated; therefore, all experiments were performed with heterozygous CAG-*ATP7A* mice and wild-type littermates were used as controls. The transgenic mice displayed no overt phenotype resulting from the expression of the human ATP7A protein. Male and female mice transmitted the transgene to their progeny, and their behavior, growth rate, and life spans were similar to those of nontransgenic littermates. Furthermore, the internal organs from nontransgenic and transgenic mice were similar in size and appearance.

Western blot analysis of transgene expression. Western blot analysis of proteins from six organs (lung, heart, liver, kidney, small intestine, and brain) was carried out as described in MATERIALS AND METHODS. The affinity-purified anti-ATP7A R17-BX antibody detected a band at about 178 kDa in most tissues of the transgenic mice, consistent with the size of ATP7A (28) (Fig. 1*B*). The same blots were stripped and reprobed with calnexin to provide an estimate of the protein loaded in each lane and to allow comparison of the levels of ATP7A with the endogenous Atp7a in transgenic and nontransgenic tissues. Atp7a was barely detectable in the nontransgenic mice, with clear signals observed only in lung, kidney, and brain. In both transgenic lines, the highest level of ATP7A was observed in the heart, with moderate expression in the kidney, small intestine, and brain. The two lines had a similar pattern of expression, except for higher expression of ATP7A in the lung of T25#5 and more ATP7A observed in the liver of the T22#2 line. It was difficult to quantify the degree of overexpression of the protein in the transgenic animals because of the low endogenous levels, so we used real-time PCR to estimate the relative expression levels.

Relative levels of ATP7A and Atp7a mRNA. Total RNA was isolated from tissues, and real-time PCR was conducted with primers that were specific for the endogenous mouse *Atp7a* and the human *ATP7A*. Table 1 shows the levels of *ATP7A* relative to *Atp7a*. In all tissues, there was considerable overexpression of ATP7A mRNA from the transgene, and the amounts were generally consistent with the pattern of expression shown in the Western blots. The relative levels of *ATP7A* mRNA to *Atp7a* mRNA were highest in the heart, with up to 200-fold increases being observed in some animals. There was considerable variation in ATP7A mRNA between animals, probably because of the mosaicism of expression (see below).

Table 1. *Relative levels of ATP7A mRNA to Atp7a mRNA*

Organ	T22#2 mice	T25#5 mice
Lung	2.6–10.3	2.1–4.0
Heart	58.7–197.5	55.3–130.4
Liver	7.3–30.1	0.4–12.6
Kidney	0.8–4.8	1.0–2.7
Small intestine	7.3–135.4	6.2–24.9
Brain	8.8–39.5	4.2–7.4

Values are ranges of mRNA levels of *ATP7A* relative to *Atp7a* in T22#2 and T25#5 mouse tissues. Four mice were examined in each group.

Immunohistochemical analysis. To detect the cellular pattern of expression of ATP7A, tissue sections were incubated with the R17-BX antibody as described in MATERIALS AND METHODS. Endogenous Atp7a was not detectable under the conditions used (Fig. 2, *A*, *D*, *G*, *J*, and *M*). In both lines, a variable mosaic expression pattern of ATP7A was observed in most tissues, and the pattern of expression differed between individual mice (data not shown). In kidney of T22#2 mice (Fig. 2*B*), ATP7A immunoreactivity was localized predominantly in tubules with a morphology consistent with that of distal tubules, whereas in T25#5, the staining was less pronounced in tubules. The immunostaining appeared in the podocytes in the glomerulus (Fig. 2*C*) and in the macula densa of the distal tubules, as well as in the thin loops of Henle and the outer medulla, but there appeared to be little staining in the proximal tubules (data not shown). Strong ATP7A immunoreactivity was detected in the perinuclear region of the enterocytes in the small intestine of both lines (Fig. 2, *E* and *F*). Transgenic protein was immunolocalized in patches in the liver hepatocytes (Fig. 2, *H* and *I*), in which endogenous Atp7a is not usually expressed (26). Interestingly, the protein appeared to be localized to the plasma membrane of hepatocytes, in contrast to the cytoplasmic perinuclear labels observed in other cell types. Immunostaining was observed in the smooth muscle cells of lung blood vessels (Fig. 2, *K* and *L*), and the cardiac muscle cells of the heart displayed strong staining (Fig. 2, *N* and *O*), consistent with the high expression noted in Western blot analysis; even in the heart, however, the mosaic expression was noted (Fig. 2, *N* and *O*). Because of the importance of the brain abnormalities in Menkes disease, we conducted a more detailed analysis of the expression pattern of the transgene in this organ in 60-day-old T22#2 and T25#5 mice. Because similar staining patterns were observed in both lines, only sections of the T22#2 line are shown (Fig. 3). Regarding the other tissues analyzed, the endogenous protein was not detected under the condition used (data not shown). Strong immunoreactivity was observed predominantly in the CA2 region of the hippocampus (Fig. 3, *A* and *B*), the Purkinje cells of the cerebellum (Fig. 3, *C* and *D*), and the choroid plexus (Fig. 3, *E* and *F*). The staining was cytoplasmic and perinuclear, consistent with the location in the *trans*-Golgi network. Immunostaining was also observed in the CA1 and CA3 regions, the dentate gyrus, and the ependymal cells of the hippocampus (data not shown).

Tissue Cu concentrations. To determine whether overexpression of human Menkes protein altered Cu homeostasis in the transgenic mice, Cu concentrations in tissues from 60- and 300-day-old normal and transgenic mice were determined using atomic absorption spectrometry. As shown in Fig. 4, the overall effect of transgenic expression was to deplete tissue Cu, an effect that became more marked as the animals aged and was most pronounced in the heart and brain. In general, the T22#2 line was more severely depleted. Cu concentrations in the heart were decreased in both young and old transgenic mice compared with normal mice, with the reduction being more pronounced in the older group, and the effect was more significant in the females. In the 300-day-old T22#2 females, the Cu concentration was decreased by 24% compared with normal females [17.61 μg/g (SD 3.47) vs. 23.23 μg/g (SD 2.09) dry wt; $P < 0.001$, Student's *t*-test]. A similar reduction in cardiac Cu was apparent in the older T25#5 females. The older T22#2 males showed an 18% reduction in Cu concentration [18.33 μg/g (SD 4.19) compared with 22.44 μg/g (SD 1.66) dry wt in nontransgenic mice; $P = 0.03$, Student's *t*-test]. Liver Cu was significantly deficient in 60-day-old T22#2 female mice [10.80 μg/g (SD 1.29) vs. 14.44 μg/g (SD 1.44) dry wt; $P < 0.001$, Student's *t*-test], but the hepatic Cu concentrations in female 60-day-old T25#5 mice was not reduced. The lowering of liver Cu was still significant in 300-day-old T22#2 females, but again, the T25#5 female hepatic Cu was the same as that in the nontransgenic group. All 60-day-old male mice had higher hepatic Cu concentrations than females of the same age; however, the transgenic mice did not differ in this respect from the nontransgenic mice. Kidney Cu concentrations were reduced in the T22#2 mice, but this reduction was significant only in the 60-day-old males and the 300-day-old females. The T25#5 line did not display a reduction in kidney Cu, perhaps because of the different pattern of expression in this organ between the two lines (Fig. 2). Small intestine Cu concentrations were slightly reduced in the older T22#2 female transgenic mice [7.85 μg/g (SD 0.75) vs. 9.48 μg/g (SD 1.29) dry wt; $P < 0.05$, Student's *t*-test], with a similar reduction in males of this age. The brains of the T22#2 transgenic animals showed marked reductions in Cu concentrations, and some reduction occurred in the T25#5 line; however, the reduction was significant only in the 300-day-old male mice of this line. Cu concentrations in the brains of 60-day-old T22#2 animals were reduced by ~23% in females [16.25 μg/g (SD 2.16) vs. 21.22 μg/g (SD 1.24) dry wt; $P < 0.001$, Student's *t*-test] and 30% in males [14.88 μg/g (SD 0.99) vs. 21.30 μg/g (SD 4.35) dry wt; $P < 0.001$, Student's *t*-test]. A similar lowering of brain Cu concentrations was apparent in the 300-day-old animals.

DISCUSSION

The two Cu ATPases in mammals, ATP7A and ATP7B, play a central role in maintaining physiological Cu balance (19). Despite the fact that these two molecules are so closely related, they clearly have distinct roles because the phenotypes in Menkes and Wilson disease are completely different. We previously proposed (20) a model of the physiological role of these proteins based on the known pattern of expression and disease phenotypes. This model envisages ATP7A being required primarily for transport of Cu across the small intestine, delivery of Cu to the brain, removal of excess Cu from cells other than hepatocytes, transport of Cu across the placenta, and delivery of Cu to a variety of secreted Cu-dependent enzymes. The Wilson protein has the major role in regulating biliary Cu excretion and delivery of Cu to ceruloplasmin.

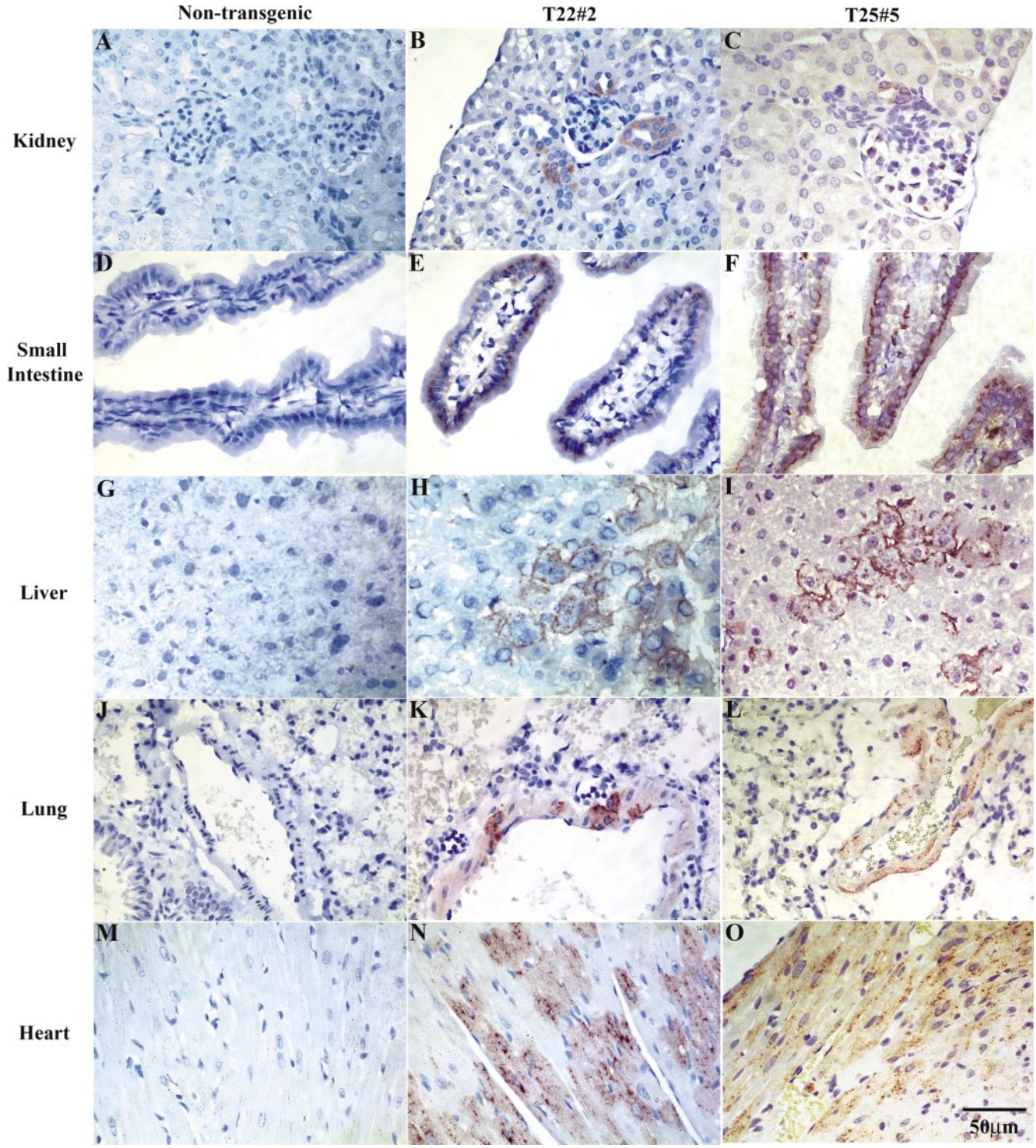

Fig. 2. Immunohistochemical analysis of transgene expression in the kidney, small intestine, liver, lung, and heart of nontransgenic, T22#2, and T25#5 transgenic mice. Strong immunoreactivity was noted in the distal tubules (*B*) and glomerulus (*C*) of kidney, the enterocytes of the small intestine (*E* and *F*), hepatocytes (*H* and *I*), the smooth muscle cells of the lung blood vessel (*K* and *L*), and cardiac muscle cells (*N* and *O*). Endogenous Atp7a was not detected in wild-type mouse tissues using this technique (*A*, *D*, *G*, *J*, and *M*).

Most studies of the Cu transport functions of ATP7A have been performed in cultured cells in which the Menkes protein was expressed at a high level to facilitate easy detection using immunofluorescence microscopy, because in many cell types, the endogenous ATP7A is too low for detailed analysis. The ATP7A-overexpressing cell lines revealed that the protein was stimulated to move from the *trans*-Golgi network to the plasma membrane when cells were exposed to elevated Cu (28). Overexpression of the protein was also found to confer Cu resistance to the cells because of enhanced ability to efflux Cu

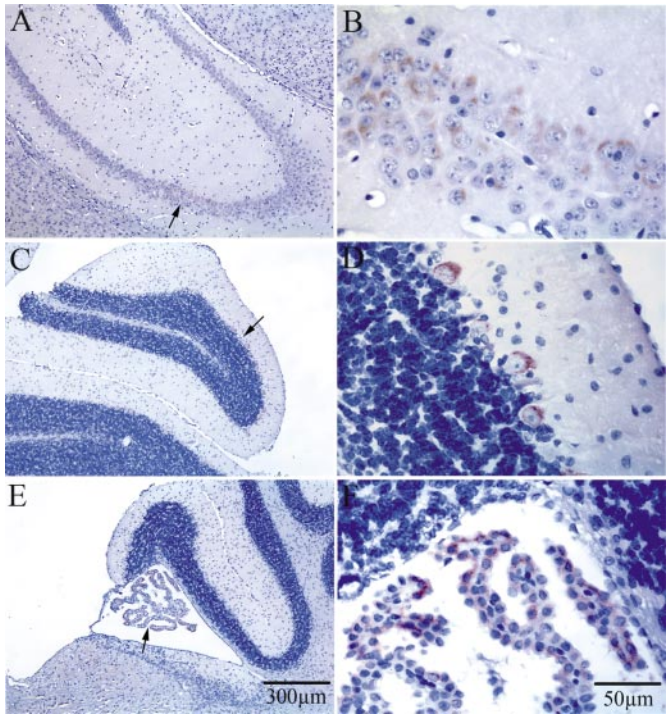

Fig. 3. Immunohistochemical analysis of transgene expression in mouse brain tissues. Strong signals were observed in the CA2 region (arrows in *A* and *B*) of the hippocampus, Purkinje cells (arrow in *C*), and choroid plexus (arrow in *E*) of the cerebellum. *B*, *D*, and *F*: higher-magnification images of sections shown in *A*, *C*, and *E*, respectively. Endogenous Atp7a was not detected in wild-type mouse brain tissues (data not shown).

(4). We proposed that Cu-induced trafficking of ATP7A represented a central homeostatic mechanism that maintains intracellular Cu levels within safe limits and suggested that this mechanism would also regulate Cu balance in the whole animal. We found that the levels of ATP7A in murine tissues are too low for studies of the localization of the protein, so the question of whether the trafficking of the Menkes protein is a physiological phenomenon could not readily be answered.

To help overcome the problems of detection and to investigate the effects of overexpression of ATP7A, we have developed some lines of transgenic mice in which the human ATP7A is expressed from the CAG promoter. Although the expression of ATP7A in the transgenic mice does not exactly match that of the endogenous Atp7a, our present results for two lines, T22#2 and T25#5, show that the expression pattern of the transgenic protein is similar to the endogenous protein, with two major differences: the Menkes protein (ATP7A) is expressed in some hepatocytes in the transgenic mice and at high levels in the heart. Messenger RNA levels estimated on the basis of real-time PCR suggested that the level of expression was highly variable between mice, and this was presumably due to the mosaic expression of the transgene that was evident from the immunocytochemical analysis. In the heart, high levels of expression (up to 197.5-fold) were detected using real-time PCR, but the relative levels of protein could not be estimated, because the endogenous protein was not detectable. Despite the increased amounts of ATP7A in cells, there did not appear to be mislocalization of the protein, because in all cells except hepatocytes, the protein appeared to be in a position

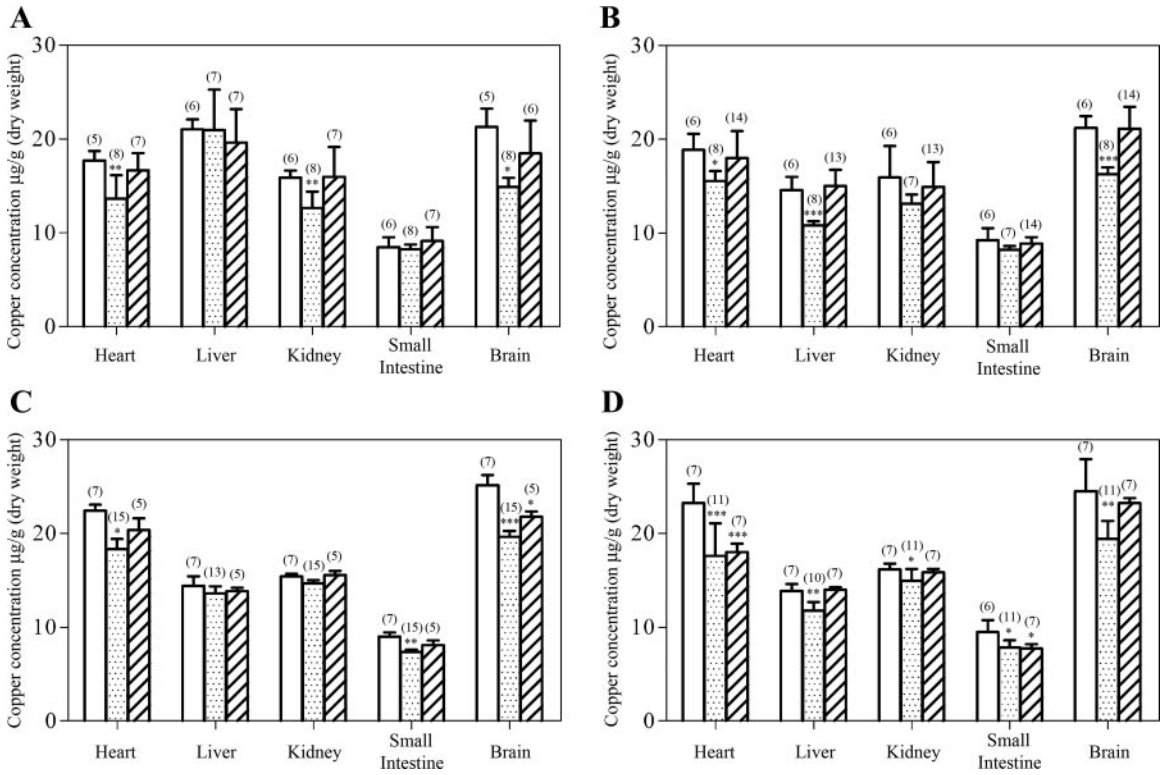

Fig. 4. Tissue Cu concentrations in nontransgenic, T22#2, and T25#5 transgenic mice. *A*: 60-day-old males. *B*: 60-day-old females. *C*: 300-day-old males. *D*: 300-day-old females. Data are means with SDs. Cu concentrations are expressed as μg/g dry wt tissue. Numbers in brackets are the number of mice examined in each group. Open bars, nontransgenic tissues; dotted bars, T22#2 transgenic tissues; bars with oblique lines, T25#5 transgenic tissues. $*P < 0.05$. $**P < 0.01$. $***P < 0.001$.

consistent with the *trans*-Golgi network in which ATP7A is found in cultured cells not exposed to Cu (28). This localization was most clearly observed with regard to the enterocytes of the small intestine (Fig. 2, *E* and *F*), where the protein is localized tightly around the serosal side of the nucleus. This tight pattern is suggestive of relatively low intracellular Cu concentration, and in other work, ATP7A was found to respond to increased dietary Cu by trafficking to the basolateral region of the enterocyte (22). The transgene is expressed in the CA2 region of the hippocampus, the choroid plexus, and Purkinje cells of the cerebellum (Fig. 3, *B*, *D*, and *F*). The expression pattern of the transgene is similar to endogenous *Atp7a* expression as shown by in situ hybridization (14, 24). The perinuclear staining in Purkinje cells is consistent with the usual *trans*-Golgi localization of ATP7A (28). The pattern of staining in hepatocytes was different, with the protein apparently localized to the plasma membrane (Fig. 2, *H* and *I*). We conclude that ATP7A is located in the basolateral surface of these hepatocytes because the markers on the apical surface (abutting the biliary canaliculus) produce a distinct circular pattern (32). This result is of interest because it provides an explanation for the normal lack of expression of ATP7A in hepatocytes. It appears that in the hepatocytes, ATP7A is localized to the plasma membrane rather than to the *trans*-Golgi network, even when mice are not Cu loaded (28). The liver has a special role in Cu homeostasis, because most newly absorbed dietary Cu is absorbed by this organ and excess Cu is excreted in the bile via the action of ATP7B (6). Thus it is probably a relatively constant influx of Cu into hepatocytes even with normal dietary intake of Cu, resulting in trafficking of ATP7A to the plasma membrane. The localization of ATP7A on the basolateral membrane has been observed in other polarized cells, such as Madin-Darby canine kidney cells in culture, but only when cells are exposed to high Cu concentrations (10). ATP7B traffics to subapical vesicles or to the apical membrane in hepatocytes (30, 32). This different trafficking pathway of the two ATPases indicates that if the Menkes protein were expressed in hepatocytes, excess Cu would be pumped back into the circulation rather than being excreted in the bile and possibly rendering the animal susceptible to Cu toxicosis. Reports in the literature on the pattern of expression of endogenous Atp7a in the kidney differ somewhat. Earlier immunohistochemical studies conducted by our group showed Atp7a in the proximal and distal tubules with slight expression in the glomeruli (11), and these results were in general agreement with in situ data published by Murata et al. (24). However, Moore and Cox (23) found that Atp7a is expressed at a high level in glomeruli, with only weak staining in some tubules. In our transgenic mice, the transgene expression was localized mainly in glomeruli in T25#5 mice and in the distal tubules in T22#2 mice, with little to no staining in the proximal tubules in either line.

To investigate whether the higher levels of expression of ATP7A produced an alteration of Cu distribution, the Cu concentrations in a range of tissues and at two age groups, young adults (60 days old) and older animals (300 days old), were determined. On the basis of the cultured cell experiments (4), we expected that the additional expression of ATP7A would produce enhanced efflux of Cu and possibly deplete tissues of Cu. The extent of this depletion, however, may have been moderated by the reduction in trafficking of the protein to the plasma membrane when cytoplasmic Cu concentrations were reduced (4). Significant depletion of Cu was observed, most notably in heart, where expression of ATP7A was highest. The depletion was a highly significant 24% in hearts of older females. Cu deficiency in mice has been shown to produce cardiac hypertrophy (9), but we did not observe any obvious cardiac abnormalities in our mice. Nevertheless, we suggest that these transgenic mice will be highly susceptible to cardiac damage when placed on a low-Cu diet. Cu concentrations in the brain of the younger T22#2 mice were reduced by 23% in females and by 30% in males. This finding is also significant because Cu levels in the brain are tightly regulated as a result of the importance of Cu for normal brain development. Severe Cu depletion observed in the mouse models of Menkes disease produces such severe neurodegeneration that the animals die by 15 days of age. Our transgenic mice clearly did not experience such severe depletion; however, as with the heart, it will be of interest to see whether the brain development of transgenic animals is more sensitive than that of normal mice to Cu depletion. Reduction in Cu in the liver was observed only in young T22#2 female mice. At first sight, this might suggest that the nonphysiological expression of ATP7A in hepatocytes does not lead to efflux of Cu into the blood as suggested above. Because the gene was expressed only in patches of hepatocytes, it is possible that an insufficient number of cells expressed the gene to produce a change in overall tissue Cu content. Nevertheless, even limited expression of ATP7A in hepatocytes may produce adverse effects if the animals are Cu loaded. We are currently investigating this possibility.

In summary, the transgenic mice show interesting disturbances of Cu homeostasis, consistent mostly with enhanced efflux capacity due to overexpression of ATP7A, and they may prove of considerable interest in further experiments in which mice are exposed to low and high Cu concentrations.

ACKNOWLEDGMENTS

We thank Dr. Sharon Ricardo, Dr. Steven Petratos, and Dr. Jane Black for assistance with kidney, heart, and brain morphology and Maree Bilandzic for reading the manuscript.

GRANTS

We thank the International Copper Association and the National Health and Medical Research Council of Australia for support of this work.

REFERENCES

1. **Ackland ML, Anikijenko P, Michalczyk A, and Mercer JFB.** Expression of Menkes copper-transporting ATPase, MNK, in the lactating human breast: possible role in copper transport into milk. *J Histochem Cytochem* 47: 1553–1562, 1999.
2. **Bull PC and Cox DW.** Wilson disease and Menkes disease: new handles on heavy-metal transport. *Trends Genet* 10: 246–252, 1994.
3. **Bull PC, Thomas GR, Rommens JM, Forbes JR, and Wilson Cox D.** The Wilson disease gene is a putative copper transporting P-type ATPase similar to the Menkes gene. *Nat Genet* 5: 327–337, 1993.
4. **Camakaris J, Petris MJ, Bailey L, Shen P, Lockhart P, Glover TW, Barcroft CL, Patton J, and Mercer JFB.** Gene amplification of the Menkes (MNK; ATP7A) P-type ATPase gene of CHO cells is associated with copper resistance and enhanced copper efflux. *Hum Mol Genet* 4: 2117–2123, 1995.
5. **Chelly J, Tümer Z, Tønnesen T, Petterson A, Ishikawa-Brush Y, Tommerup N, Horn N, and Monaco AP.** Isolation of a candidate gene for Menkes disease that encodes a potential heavy metal binding protein. *Nat Genet* 3: 14–19, 1993.

6. **Cox DW.** Genes of the copper pathway. *Am J Hum Genet* 56: 828–834, 1995.
7. **Critchley HOD, Wang H, Kelly RW, Gebbie AE, and Glasier AF.** Progestin receptor isoforms and prostaglandin dehydrogenase in the endometrium of women using a levonorgestrel-releasing intrauterine system. *Hum Reprod* 13: 1210–1217, 1998.
8. **Danks DM.** Disorders of copper transport. In: *Metabolic and Molecular Basis of Inherited Disease* (7th ed.), edited by Scriver CR, Beaudet AL, Sly WS, and Valle D. New York: McGraw-Hill, 1995, vol. I, pt. 10, p. 2211–2235.
9. **Elsherif L, Wang L, Saari JT, and Kang YJ.** Regression of dietary copper restriction-induced cardiomyopathy by copper repletion in mice. *J Nutr* 134: 855–860, 2004.
10. **Greenough M, Pase L, Voskoboinik I, Petris MJ, Wilson O'Brien A, and Camakaris J.** Signals regulating trafficking of the Menkes (MNK; ATP7A) copper-translocating P-type ATPase in polarized MDCK cells. *Am J Physiol Cell Physiol* 287: C1463–C1471, 2004.
11. **Grimes A, Hearn C, Lockhart P, Newgreen D, and Mercer JFB.** Molecular basis of the brindled mouse mutant (*Mo^{br}*): a murine model of Menkes disease. *Hum Mol Genet* 6: 1032–1042, 1997.
12. **Hardman B, Manuelpillai U, Wallace EM, van de Waasenburg S, Cater M, Mercer JFB, and Ackland ML.** Expression and localization of Menkes and Wilson copper transporting ATPases in human placenta. *Placenta* 25: 512–517, 2004.
13. **Horn N.** Copper incorporation studies on cultured cells for prenatal diagnosis of Menkes' disease. *Lancet* 1: 1156–1158, 1976.
14. **Iwase T, Nishimura M, Sugimura H, Igarashi H, Ozawa F, Shinmura K, Suzuki M, Tanaka M, and Kino I.** Localization of Menkes gene expression in the mouse brain: its association with neurological manifestations in Menkes and model mice. *Acta Neuropathol (Berl)* 91: 482–488, 1996.
15. **Kosonen T, Uriu-Hare JY, Clegg MS, Keen CL, and Rucker RB.** Incorporation of copper into lysyl oxidase. *Biochem J* 327: 283–289, 1997.
16. **La Fontaine S, Firth SD, Lockhart PJ, Brooks H, Parton RG, Camakaris J, and Mercer JFB.** Functional analysis and intracellular localization of the human Menkes protein (MNK) stably expressed from a cDNA construct in Chinese hamster ovary cells (CHO-K1). *Hum Mol Genet* 7: 1293–1300, 1998.
17. **Linder MC.** *Biochemistry of Copper*. New York: Plenum, 1991.
18. **Linder MC, Wooten L, Cerveza P, Cotton S, Shulze R, and Lomeli N.** Copper transport. *Am J Clin Nutr* 67, *Suppl* 5: 965S–971S, 1998.
19. **Llanos RM and Mercer JFB.** The molecular basis of copper homeostasis copper-related disorders. *DNA Cell Biol* 21: 259–270, 2002.
20. **Mercer JFB, Kramer D, and Camakaris J.** Molecular basis of diseases of copper homeostasis. In: *Handbook of Copper Pharmacology and Toxicology*, edited by Massaro EJ. Totowa, NJ: Humana, 2002, p. 249–276.
21. **Mercer JFB, Livingston J, Hall B, Paynter JA, Begy C, Chandrasekharappa S, Lockhart P, Grimes A, Bhave M, Siemieniak D, and Glover TW.** Isolation of a partial candidate gene for Menkes disease by positional cloning. *Nat Genet* 3: 20–25, 1993.
22. **Monty F, Llanos RM, Mercer JFB, and Kramer DR.** Copper exposure induces trafficking of the Menkes protein in intestinal epithelium of ATP7A transgenic mice. *J Nutr* 135: 2762–2766, 2005.
23. **Moore SDP and Cox DW.** Expression in mouse kidney of membrane copper transporters Atp7a and Atp7b. *Nephron* 92: 629–634, 2002.
24. **Murata Y, Kodama H, Abe T, Ishida N, Nishimura M, Levinson B, Gitschier J, and Packman S.** Mutation analysis and expression of the mottled gene in the macular mouse model of Menkes disease. *Pediatr Res* 42: 436–442, 1997.
25. **Niwa H, Yamamura K, and Miyazaki J.** Efficient selection for high-expression transfectants with a novel eukaryotic vector. *Gene* 108: 193–199, 1991.
26. **Paynter JA, Grimes A, Lockhart P, and Mercer JFB.** Expression of the Menkes gene homologue in mouse tissues lack of effect of copper on the mRNA levels. *FEBS Lett* 351: 186–190, 1994.
27. **Petris MJ and Mercer JFB.** The Menkes protein (ATP7A, MNK) cycles via the plasma membrane in basal and elevated extracellular copper using a C-terminal di-leucine endocytic signal. *Hum Mol Genet* 8: 2107–2115, 1999.
28. **Petris MJ, Mercer JFB, Culvenor JG, Lockhart P, Gleeson PA, and Camakaris J.** Ligand-regulated transport of the Menkes copper P-type ATPase efflux pump from the Golgi apparatus to the plasma membrane: a novel mechanism of regulated trafficking. *EMBO J* 15: 6084–6095, 1996.
29. **Petris MJ, Strausak D, and Mercer JFB.** The Menkes copper transporter is required for the activation of tyrosinase. *Hum Mol Genet* 9: 2845–2851, 2000.
30. **Roelofsen H, Wolters H, Van Luyn MJA, Miura N, Kuipers F, and Vonk RJ.** Copper-induced apical trafficking of *ATP7B* in polarized hepatoma cells provides a mechanism for biliary copper excretion. *Gastroenterology* 119: 782–793, 2000.
31. **Schaefer M, Hopkins RG, Failla ML, and Gitlin JD.** Hepatocyte-specific localization and copper-dependent trafficking of the Wilson's disease protein in the liver. *Am J Physiol Gastrointest Liver Physiol* 276: G639–G646, 1999.
32. **Schaefer M, Roelofsen H, Wolters H, Hofmann WJ, Müller M, Kuipers F, Stremmel W, and Vonk RJ.** Localization of the Wilson's disease protein in human liver. *Gastroenterology* 117: 1380–1385, 1999.
33. **Tanzi RE, Petrukhin K, Chernov I, Pellequer JL, Wasco W, Ross B, Romano DM, Parano E, Pavone L, Brzustowicz LM, Devoto M, Peppercorn J, Bush AI, Sternlieb I, Pirastu M, Gusella JF, Evgrafov O, Penchaszadeh GK, Honig B, Edelman IS, Soares MB, Scheinberg IH, and Gilliam TC.** The Wilson disease gene is a copper transporting ATPase with homology to the Menkes disease gene. *Nat Genet* 5: 344–350, 1993.
34. **Terada K, Nakako T, Yang XL, Iida M, Aiba N, Minamiya Y, Nakai M, Sakaki T, Miura N, and Sugiyama T.** Restoration of holoceruloplasmin synthesis in LEC rat after infusion of recombinant adenovirus bearing *WND* cDNA. *J Biol Chem* 273: 1815–1820, 1998.
35. **Thomas GR, Forbes JR, Roberts EA, Walshe JM, and Cox DW.** The Wilson disease gene: spectrum of mutations and their consequences. *Nat Genet* 9: 210–217, 1995.
36. **Tümer Z, Møller LB, and Horn N.** Mutational spectrum of *ATP7A*, the gene defective in Menkes disease. *Adv Exp Med Biol* 448: 83–95, 1999.
37. **Vulpe C, Levinson B, Whitney S, Packman S, and Gitschier J.** Isolation of a candidate gene for Menkes disease and evidence that it encodes a copper-transporting ATPase. *Nat Genet* 3: 7–13, 1993.
38. **Wang RF and Kushner SR.** Construction of versatile low-copy-number vectors for cloning, sequencing and gene expression in *Escherichia coli*. *Gene* 100: 195–199, 1991.
39. **Yamaguchi Y, Heiny ME, and Gitlin JD.** Isolation and characterization of a human liver cDNA as a candidate gene for Wilson disease. *Biochem Biophys Res Commun* 197: 271–277, 1993.